

PAPER

Framework for assessment of magnetic equilibrium controller performance on the MAST upgrade spherical tokamak

To cite this article: A Lvovskiy et al 2025 Plasma Phys. Control. Fusion 67 075003

View the <u>article online</u> for updates and enhancements.

You may also like

- Data driven prediction of the neutral gas pressure in the stellarator Wendelstein 7-X D Angelis, F Sofos, S Misdanitis et al.
- Nonlinear evolution of ideal pressuredriven MHD modes and their conversion into tearing-type modes
 J Ma, W Guo and Q Yu
- Tomography of divertor neutral particle emission using visible CCD imaging under metal-wall condition in EAST Beihe Zhang, Qingquan Yang, Baoguo Wang et al.

Plasma Phys. Control. Fusion 67 (2025) 075003 (10pp)

https://doi.org/10.1088/1361-6587/ade3fd

Framework for assessment of magnetic equilibrium controller performance on the MAST upgrade spherical tokamak

A Lvovskiy^{1,*}, H Anand¹, A S Welander¹, M Kochan², C Vincent², G McArdle², J Lovell³, Z A Xing¹, J L Barr¹, E Cho¹, B Sammuli¹, D A Humphreys¹, N W Eidietis¹, V Soukhanovskii⁴, A W Leonard¹, A O Nelson⁵, A Thornton² and J Harrison²

E-mail: lvovskiya@fusion.gat.com

Received 28 March 2025, revised 4 June 2025 Accepted for publication 12 June 2025 Published 20 June 2025



Abstract

In this work we present the assessment framework for magnetic equilibrium controllers on MAST Upgrade spherical tokamak (MAST-U) spherical tokamak. Such controllers are essential for the MAST-U since exhaust physics and core-edge integration studies require advanced divertor plasma configurations. The developed framework is based on the TokSys suite of plasma control codes, which was adapted and upgraded for MAST-U. However, extra capabilities were added on top of TokSys to support the development of new control algorithms, deployment of controllers to the plasma control system (PCS) and evaluation of their performance. The controller assessment was realized via closed-loop integrated control simulations with the actual MAST-U PCS and different physics-based plasma models. Since all components of the assessment chain were experimentally validated, these simulations provide qualified controllers applicable for direct use in the experiment. This resulted in the successful experimental demonstration of advanced plasma shape control on MAST-U with minimal on-machine development time. A similar methodology would be beneficial to other tokamaks, both existing and future.

Keywords: plasma shape control, controller assessment, discharge simulation

1. Introduction

The MAST Upgrade spherical tokamak (MAST-U) is designed with large outer divertors to study how the flux expansion and/or divertor leg extention can allow increased plasma core power density in addition to reducing the erosion or damage of the divertor target [1]. This assumes exploration

of various magnetic configurations, including the Super-X divertor geometry, characterized by a very distant strike point with a greatly increased plasma-wetted area (see figure 1) [2]. On this route, every new magnetic configuration requires development of its own set of magnetic shape controllers. Initially, MAST-U was lacking capabilities to test shape controllers before the experiment and relied on their tuning and debugging during operations. To reduce the on-machine time required for the shape controller commissioning, we have developed a controller assessment framework for MAST-U.

¹ General Atomics, PO Box 85608, San Diego, CA, United States of America

² United Kingdom Atomic Energy Authority, Abingdon, United Kingdom

³ Oak Ridge National Laboratory, Oak Ridge, TN, United States of America

⁴ Lawrence Livermore National Laboratory, Livermore, CA, United States of America

⁵ Columbia University, New York City, NY, United States of America

^{*} Author to whom any correspondence should be addressed.

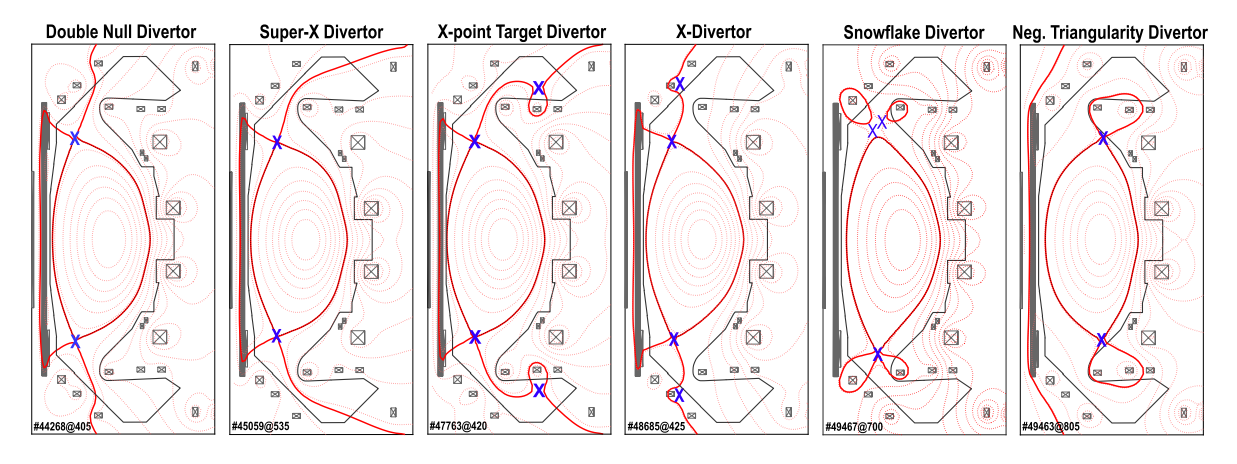


Figure 1. Magnetic configurations enabled on MAST-U with the controller assessment framework. See figure 2 for geometric dimensions.

Presently, this framework is extensively used to design, simulate and assess the performance of magnetic shape controllers off-line before applying them in the real experiment. All MAST-U magnetic configurations shown in figure 1 have been made possible due to this framework [3–6].

The developed framework is based on the TokSys suite of codes (short for Tokamak System toolbox, it provides control development and analysis tools [7]), with extra capabilities added on top to assess the performance of shape controllers and ease their implementation to the MAST-U plasma control system (PCS). There are codes in the tokamak community allowing simulation of the plasma discharge and some validation of plasma controllers (often called flight or tokamak simulators), for example, FENIX for ASDEX Upgrade [8], MEQ for TCV [9], and SOPHIA for ST40 [10]. However, this is a first-of-a-kind controller assessment framework available for MAST-U. The presented assessment approach also follows the principles laid down by ITER [11, 12], making it one of the first demonstrations of the ITER method on an existing machine.

The structure of the paper is organized as follows. In section 2 we discuss the requirements for magnetic controllers on MAST-U, in section 3 we present the controller validation and assessment framework, and in section 4 we provide an example of a qualified controller application in the real experiment.

2. Requirements for magnetic shape controllers on MAST-U

The requirements for magnetic shape controllers are closely tied to the MAST-U magnetic system and plasma shape reconstruction, thus we briefly introduce them below before listing controller design and performance requirements.

The MAST-U magnetic system consists of a central solenoid (P1), two main symmetric coil pairs to provide equilibrium and shaping (P4 and P5), one anti-symmetric coil pair for the vertical control (P6), a solenoidal coil to flatten the inner plasma shape (Pc, installed but not commissioned), and

8 coil pairs in the divertor region to realize various divertor magnetic configurations (D1, D2, D3, D5, D6, D7, Dp, Px), see figure 2(left) [13].

The real-time equilibrium reconstruction on MAST-U is made by the Local Expansion MAST Upgrade Reconstruction code (LEMUR [14, 15]). LEMUR, unlike EFIT, provides only a limited set of parameters including the outer plasma boundary radius at the midplane (R_{OUT}), inner boundary radius at the midplane (R_{IN}), coordinates of the lower X-point (R_X , Z_X), radial coordinate of the strike point (R_{STK}), flux expansion at the strike target point ($f_{exp,t}$), the so-called nose gap (N_g) and throat gap (T_g), as shown in figure 2(right).

Magnetic shape controllers for MAST-U by design must be able to: (1) control the shape parameters provided by LEMUR, (2) decouple responses between these control variables, (3) mainly use the Px coil to control R_{IN} , R_X until the Pc coil is commissioned, (4) be decoupled from both the plasma current control and vertical stabilization. At present, the plasma current and shape control are not decoupled, and we rely on the plasma current controller already implemented in the PCS to compensate for any perturbations introduced by the shape control. In principle, the change in magnetic flux at the plasma boundary caused by the poloidal coils can be included in the plant response matrix and accounted for in the design of actuators. This would decouple shape control from plasma current control, but it remains to be tested in future campaigns. The plasma vertical stabilization and shape control are naturally decoupled owing to their different timescales: the vertical stabilization is done on the smallest time scale ≤ 1 ms by a vertical controller outside of the PCS, while the plasma shape control is done on a larger time scale by the PCS under assumption of the stable vertical position. This approach is known as a frequency separation.

The performance of magnetic controllers must be sufficient to: (1) provide reasonable tracking with responses to step and ramp trajectories, (2) result in a small steady-state error (about 1 cm or less), (3) enable fast settling response time (about 100 ms). A small transient error was not requested by the MAST-U team since the main physics studies are during the plasma current flattop phase with a stable plasma shape.

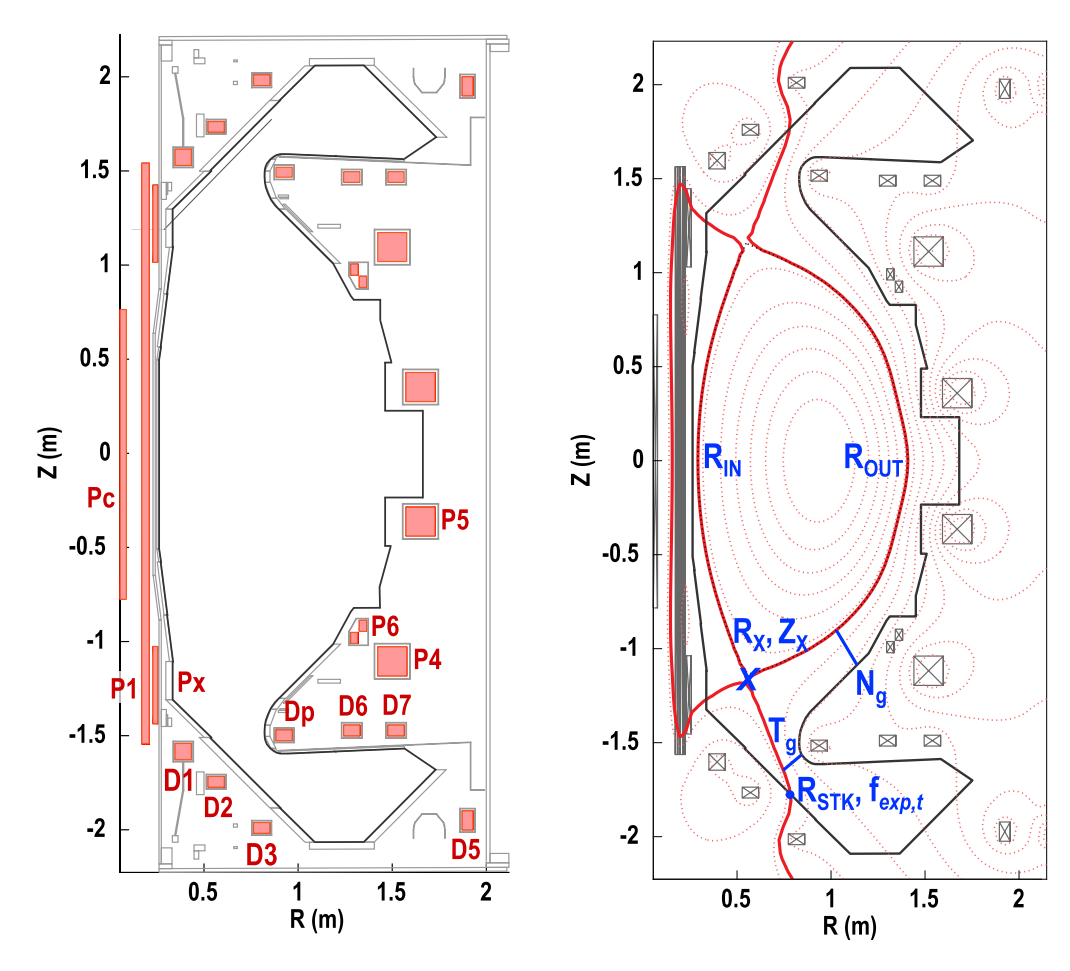


Figure 2. (left) Poloidal magnetic field coils on MAST-U; (right) controlled parameters of the MAST-U magnetic configuration, see explanation in section 2.

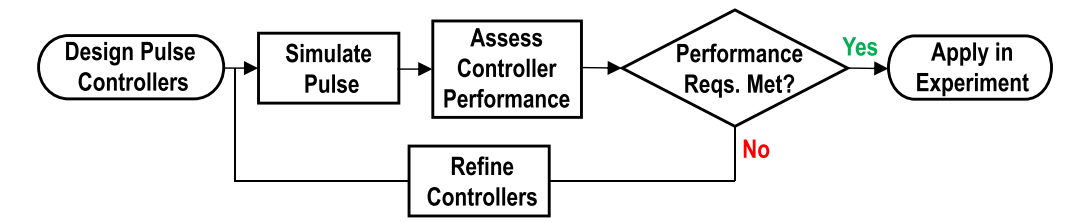


Figure 3. The workflow of the MAST-U controller assessment framework. 'Regs.' in the diamond shape is a short form of 'requirements'.

3. Framework for verification and assessment of controllers

3.1. Framework description

The controller assessment framework enables high confidence operation at high performance via providing an iterative workflow and sequential process to produce controllers meeting the user-defined targets. The workflow is shown in figure 3, it consists of (1) design of shape controllers, (2) self-consistent simulation of the plasma pulse, (3) validation and assessment of the controller performance. This process repeats with refined controller algorithms until the required controller performance is met. After that new controllers are considered qualified and applicable in the experiment.

The pulse simulator in this workflow utilizes the TokSys codes adapted for MAST-U. Its description and validation are given in section 3.3. The design and assessment of controllers are components specifically developed to complement the pulse simulator and realize the MAST-U assessment framework. The design of controllers is done using the approach presented in section 3.2. The assessment of controllers is presented in section 3.4.

3.2. Shape control algorithm

In the development of plasma shape controllers, i.e. in the design of responses of poloidal magnetic field coils actuating the desired parameter of a given magnetic configuration, we employ the approach detailed in reference [3]. Briefly, the

original plant matrix used for the shape control, i.e. calculated for specific magnetic equilibrium and linking the coil currents with controlled parameters, is complemented with a compensator (pseudo-inverse) matrix in such a way that their product is a diagonal matrix. This makes the response system decoupled and provides orthogonal sets of coils responsible for actuation of set-specific single controlled parameters. As a result, the controllers required to control a new diagonal plant matrix are much simplified. The gains of these controllers can be found via simulations and, if needed, finally tuned in the experiment.

It is important to mention that this control approach is valid only around the linearized equilibrium, i.e. the robust control of a significantly different magnetic configuration requires a development of a new controller. Also, the number of controlled parameters cannot exceed the number of coils, but the user is able to select a set of coils and parameters to control. As a final note, the columns of the pseudo-inverse matrix are often referred to as 'virtual circuits' on MAST-U [13], reflecting the fact that they help to organize physical coil currents into virtual circuits controlling only one parameter of interest. These virtual circuits can be loaded as configuration files into the MAST-U PCS to enable magnetic control of a specific plasma configuration. A set of codes was developed to design such virtual circuits based on the user-provided requirements, test them in a static way by applying a small perturbation, and generate controller configuration files suitable for import to the MAST-U PCS.

Based on this approach, we provide feedback control of parameters R_{OUT} , R_{IN} , R_X , Z_X , and R_{STK} , and feedforward control of T_g , N_g , and $f_{exp,t}$ in the experiment. Notably, not all these parameters are controlled at the same time since this may cause too high current requests in the coils depending on specific shape and plasma parameters, which is not allowed due to possible coil current saturation, limits on the total generated heat, $I_c^2 t$, and limits on the electromagnetic vertical force between coils. Also, only parameters in the lower half of the vessel are controlled under assumption of the poloidal field coil currents' symmetry. For MAST-U, the feedback control means control based on the minimization of the error between the target and controlled parameter, while the feedforward control means change of the controlled parameter during the discharge by a certain pre-programmed value (but not direct programming of the coil currents).

3.3. Pulse simulator and its validation

The pulse simulator is one of the key components of the controller assessment framework. It enables the connection of a MAST-U device model to the MAST-U PCS used in the real experiment and facilitates the execution of closed-loop discharge simulations. By implementing different controllers to the MAST-U PCS their performance can be tested and verified in simulations before confidently applying them in the experiment. For this approach to work, the MAST-U model needs to

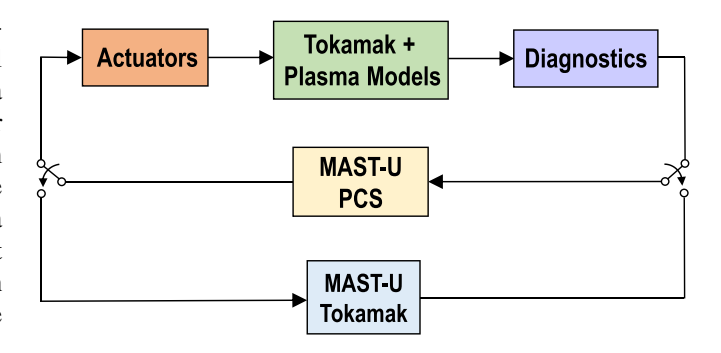


Figure 4. The layout of MAST-U pulse simulator.

be validated first against experimental data. Below we describe this model and its validation.

The device model layout (as well as the pulse simulator loop) is shown in figure 4. It includes the model of actuators, the electromagnetic model of the tokamak coupled with plasma models, and the model of diagnostics. All of these are implemented as Simulink blocks and can be connected to the MAST-U PCS via interface codes.

The *model of actuators* may include the models of power supplies, heating and current drive system, gas injection, etc but for MAST-U it presently includes only the power supplies. The implemented power supply model is relatively simple but sufficient for control needs, consisting of a delay, a first-order transfer function, and an offset, as shown in figure 5(a). The model was validated against the experiment by using real power supply voltage request commands in vacuum discharges and comparing the simulated output voltages with real output voltages. The result shows good agreement as presented in figures 5(b) and (c).

The *electromagnetic tokamak model* contains the geometry of the vacuum vessel, poloidal field coils, passive conductors as well as their resistances, inductances, mutual inductances, and Green's functions. The model of the poloidal field coils and vacuum vessel was validated by supplying real voltages in vacuum discharges and comparing driven (for coils) and induced (for vacuum vessel) currents in simulations and real discharges. We do not show these timetraces considering them trivial, and instead provide below a validation of both the electromagnetic and plasma models by simulating the vertical instability growth rate. However, we should note that validation of the electromagnetic model in vacuum discharges allowed us to refine the initial coil model by including extra resistances and inductances to take into account feed conductors and joints between the coils and power supplies.

The diagnostic block is the last hardware-specific component of the device model. It is primarily used to organize the output signals of the electromangetic model (since the electromagnetic model already contains relevant mutual inductances and Green's functions) into the groups of flux loops, magnetic probes, Rogowski coils, and prepare the diagnostic signals to be used in the closed-loop simulation environment (i.e. to be in agreement with inputs required

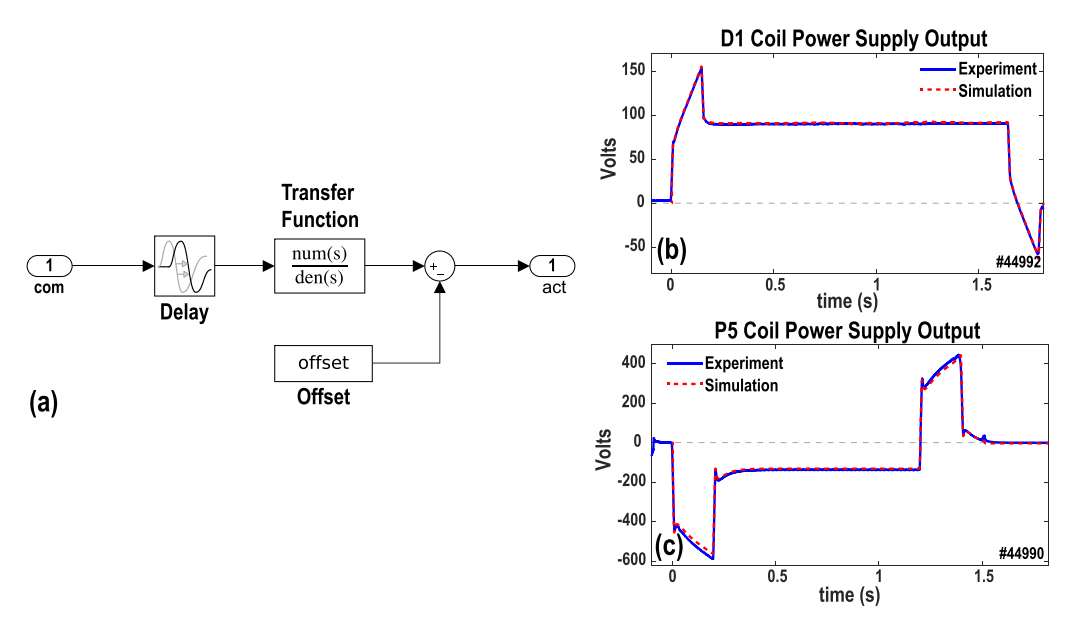


Figure 5. (a) Block scheme of the power supply model. Presently offsets for all power supplies are set to zero; (b) and (c) simulated and real voltage outputs of power supplies for D1 and P5 coils.

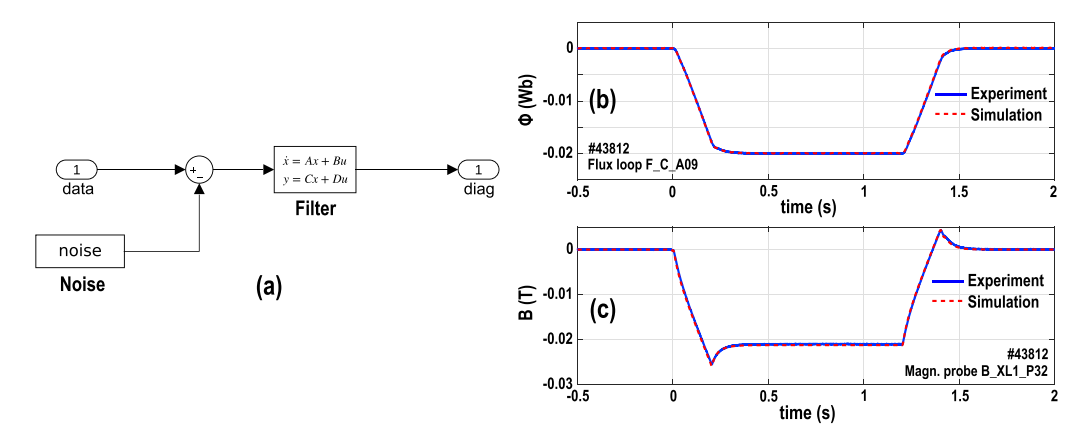


Figure 6. (a) Scheme of the Simulink diagnostic block, (b) and (c) simulated and real responses of a flux loop and a magnetic probe in a MAST-U vacuum discharge.

by the PCS). The diagnostic block also includes a noise addition block and first-order filters to turn the ideal diagnostic signals into more realistic signals using a state-space representation, see figure 6(a), though at the moment this additional functionality is yet to be commissioned. The model of diagnostics was validated against the experiment by supplying real poloidal field coil currents in vacuum discharges and comparing simulated diagnostic signals with real signals. The results show good agreement as presented in figures 6(b) and (c).

To enable tokamak plasma simulations, the device model is combined with physics-based *plasma models*. Presently, there are linear and quasi-linear plasma models available in TokSys. The linear plasma response model is computationally fast and includes both rigid plasma shape response [16] and deformable response models [17]. However, it is only valid around the equilibrium linearization time, i.e. it does not support complex plasma shape simulations like transition from positive to negative triangularity shape or full discharge evolution.

The quasi-linear model (also known as the GSevolve model) solves and evolves the free-boundary Grad–Shafranov equilibrium following prediscribed targets (those are typically plasma current or magnetic flux, plasma beta, and internal inductance) [18, 19]. It is piece-wise linear with the plasma evolving linearly until a significant change of the plasma shape (magnetic flux) triggers a non-linear update of the plasma response. This allows the GSevolve model to simulate the full discharge evolution, from the breakdown to the termination. As a trade-off, it is more computationally demanding than the linear model and takes about 10 min to simulate 1 s of the discharge using Intel Xeon Gold 6136. Typically, the linear model is used to assess controllers during a single phase of the plasma evolution, while the GSevolve model is used to study a series of plasma equilibrium phases.

As an example of the electromagnetic model and plasma model validation, we provide comparison of measured and modeled vertical instability growth rates. The measured open-loop growth rate, γ , was obtained in a discharge with a

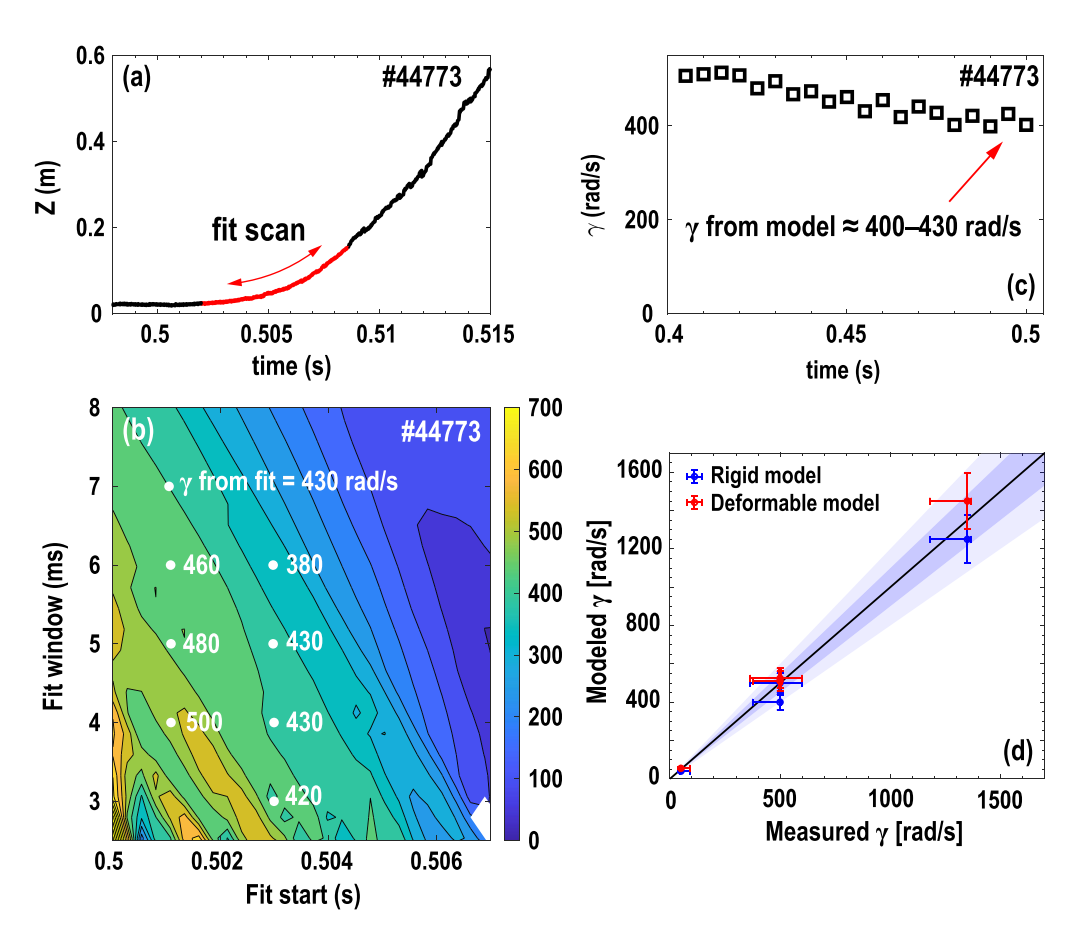


Figure 7. (a) Evolution of the plasma vertical position, Z(t), during a VDE and an example of the fit to data; (b) range of the vertical instability growth rates, γ , obtained for different fit windows of Z(t) in panel (a). Selected are γ with minimal fit residuals (residuals are not shown); (c) γ from the linear rigid model; (d) range of experimental and modeled γ in VDE discharges with small, medium and large γ . Shaded areas show up to 10% and 20% deviation from the ideal 1:1 match.

vertical displacement event (VDE) deliberately triggered by disabling MAST-U vertical control system at 0.5 s. This γ was calculated by fitting the plasma vertical position (see figure 7(a)) using different fit windows and different fit start times to get a range of growth rates observed during the VDE. As shown in figure 7(b), the experimental γ is about 380–500 rad s⁻¹. The modeled open-loop γ was calculated using the linear rigid model and eigenvalues of the system dynamic matrix (often denoted matrix A in the state-space representation). This modeled γ is shown in figure 7(c) for a number of equilibria provided by EFIT. By the moment of the VDE the modeled γ is about 400–430 rad s⁻¹. These modeled and experimental γ are in a good agreement, assuming 10% error in the model. In a similar way both experimental and modeled γ were analyzed in other MAST-U VDE discharges, as shown in figure 7(d). This additional analysis resulted in a wide range of observed γ , from about 50 rad s⁻¹ to about 1500 rad s⁻¹, which were also in a good agreement with the model. Notably, figure 7(d) presents γ from both linear rigid and linear deformable models. This comparison confirms that both the MAST-U electromagnetic model and linear plasma model are adequate in reproducing the experiment.

3.4. Assessment of a shape controller

In this subsection we assess the shape controllers for a double null diverted plasma using a typical experimental scenario, all available plasma models, and also the response to a step command. This will show that the performance of controllers is sufficient as well as include validation of the previously mentioned linear deformable and quasilinear (GSevolve) plasma models. It will also provide us with a qualified controller applicable to be used in the experiment.

For this task, we present a case where control of plasma shape parameters R_{IN} , R_{OUT} , Z_X , R_X is first assessed offmachine using closed-loop simulations and later shown in a real experiment (section 4). As a first step, these controllers were implemented in the form of virtual circuits, as discussed in section 3.2, for a double null plasma equilibrium, similar to the shape in figure 2(right). Then these controllers were added to the MAST-U PCS with R_{IN} , R_{OUT} , Z_X controlled in feedback and R_X having no programmed control but included during the generation of the virtual circuits to test the decoupling of controllers. Using the pulse simulator capabilities, the PCS was connected in closed-loop to the MAST-U device

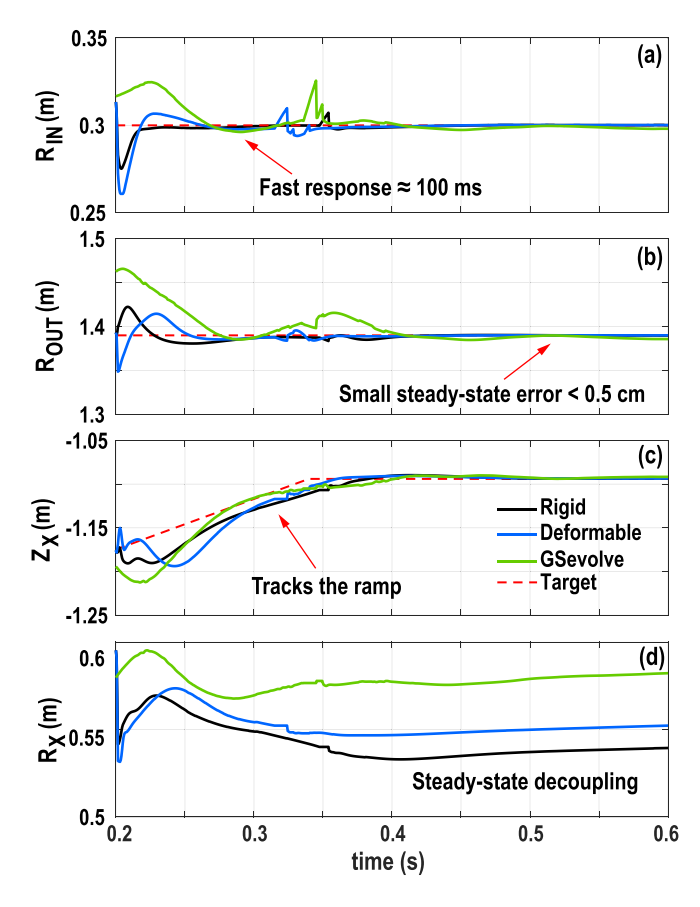


Figure 8. Closed-loop simulations of controllers for parameters R_{IN} , R_{OUT} , Z_X using linear rigid, linear deformable and GSevolve plasma response models for a double null divertor magnetic configuration on MAST-U. R_X was not controlled in the simulation, it is provided to demonstrate decoupling with other parameters. No other plasma shape parameters were controlled or requested to be decoupled in this case.

model with three different plasma models: linear rigid, linear deformable, and GSevolve models. The result of these simulations is shown in figure 8. It can be seen that all three models exhibit fast responses (\approx 100 ms), small steady-state errors (< 0.5 cm), reasonable target tracking during the ramp of Z_X (average error < 1 cm, however, this was not a quantified design requirement), as well as a steady-state decoupling seen in the panel for R_X (the decoupling is supported by about the same initial and post-transition final values of R_X). This confirms that both the shape controllers and plasma models work properly.

To further assess the performance of controllers, their response to a step command was studied. As an example, the responses of the linear rigid and GSevolve models to a -5 cm step in $R_{\rm OUT}$ target are shown in figures 9(a) and (b). It can be seen that both the linear and GSevolve models quickly react to the step command and have a settling time of about 90 ms and 120 ms respectively, which satisfies the controller performance requirement listed in section 2. The steady-state error is less than 1 mm and less than 5 mm for the linear and GSevolve models respectively, which also satisfies the controller performance requirement. Additionally, for

the case of the linear rigid model the controller performance was studied for plasmas with different resistances, namely, of basic 1.2 $\mu\Omega$ and modified by -40% and +40%. In all these cases the controller performance is almost the same, as seen in figure 9(a). To confirm that a change in the plasma resistance is acknowledged by the linear plasma model, the currents in coils P1 (central solenoid) and D1 (a coil at the entrance to the divertor) are also shown. As mentioned earlier, plasma current control and shape control are not decoupled at present. The existing plasma current controller in the MAST-U PCS utilizes the P1 coil as the sole actuator for controlling the plasma current. This explains the observation in figure 9(c) that a higher plasma resistance leads to an increased demand in the P1 coil to achieve the same plasma current reference. The shape control uses all coils except P1 and P6 and as an example of one coil from the full set used for shape control, the figure 9(d) shows D1 current evolution to track R_{OUT} reference with baseline, low, and high plasma resistances. As expected, the shape controller demands a larger current in the case when the plasma resistance is high as it needs to drive more flux as compared to the reference case to reach the same R_{OUT} reference.

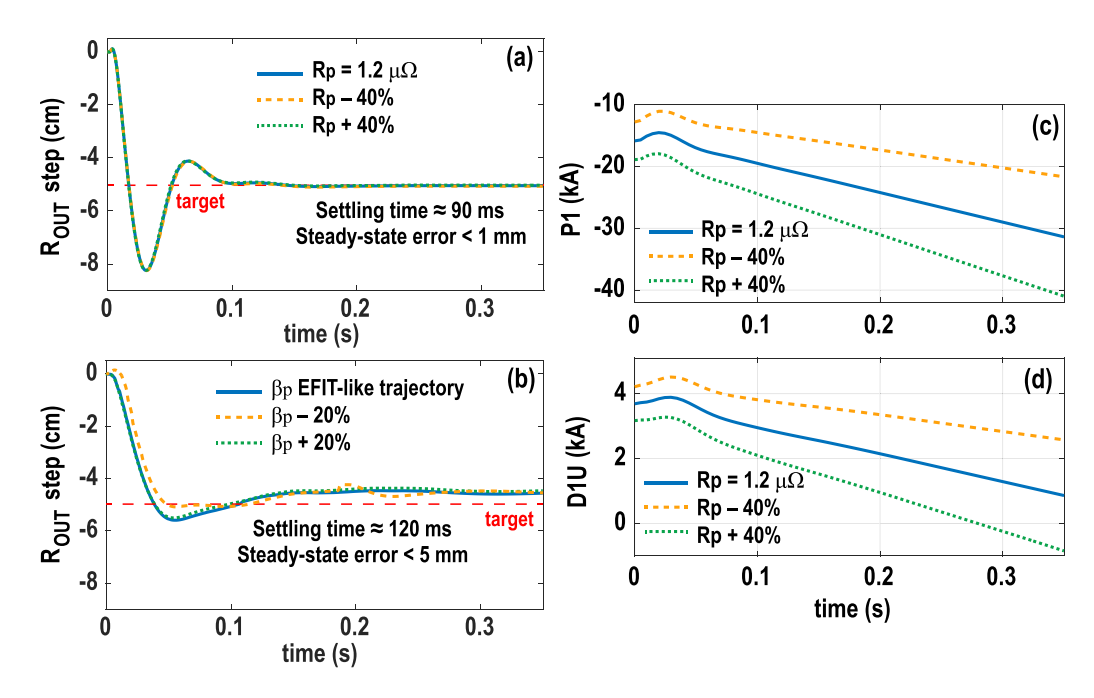


Figure 9. Controller performance assessed by applying a -5 cm step to R_{OUT} target using (a) linear rigid and (b) GSevolve plasma models. To study the robustness of the controller to a change of plasma parameters, (a) shows cases of plasma with different resistance and (b) with different plasma beta. (c), (d) Currents in coils P1 and D1 for the case shown in panel (a). The time is with respect to the beginning of the step.

A similar exercise, where a step change in R_{OUT} is studied for different plasmas, has been done using the GSevolve model. In this case the plasma beta, β_P , was changed by -20% and +20% compared to a typical EFIT trajectory of β_P for a double null plasma. As seen in figure 9(b), the controller responses also have close dynamics despite different plasma parameters. The greater steady-state error in the case of a GSevolve model is explained by the different plasma model itself and by the lack of the integral gain (it is typically set to zero during the real experiment).

This set of validations (1) completes the validation of plasma models, (2) shows the robustness of developed plasma shape controllers to the change of plasma parameters, such as resistance and beta, and (3) demonstrates how the assessment of controllers results in a qualified controller, applicable for a real experiment.

4. Application of a qualified controller in the experiment

In this section we take the plasma shape controllers developed and assessed in section 3 for a double null plasma and apply them in a real experiment. As a reminder, $R_{\rm IN}$, $R_{\rm OUT}$, Z_X

are controlled in feedback and R_X has no control, but is included in the set of controllers to show their decoupling. The timetraces of $R_{\rm IN}$, $R_{\rm OUT}$, Z_X , R_X presented in figure 10 show the comparison between the experiment and the prior GSevolve simulation. There is a good agreement both between them and the target, particularly after the plasma shape changes from the limited shape to the double null diverted shape during the plasma current ramp since the controllers were developed for the diverted plasma (the plasma diverts at about 0.12 s, the controllers were produced for the equilibrium achieved at 0.3 s). The relatively large error seen between GSevolve, experiment, and target traces during the transient phase can be explained by (1) no feed-forward control enabled during the early transient phase and (2) controllers enabled during the later transient phase were designed for the plasma equilibrium during the steady-state phase, which is primarily used for physics studies. This successful application of the qualified controllers demonstrates the power of the controller assessment framework based on experimentally validated physics-based models and closed-loop simulations with the MAST-U PCS. Similar work was performed to develop other magnetic configurations on MAST-U shown in figure 1.

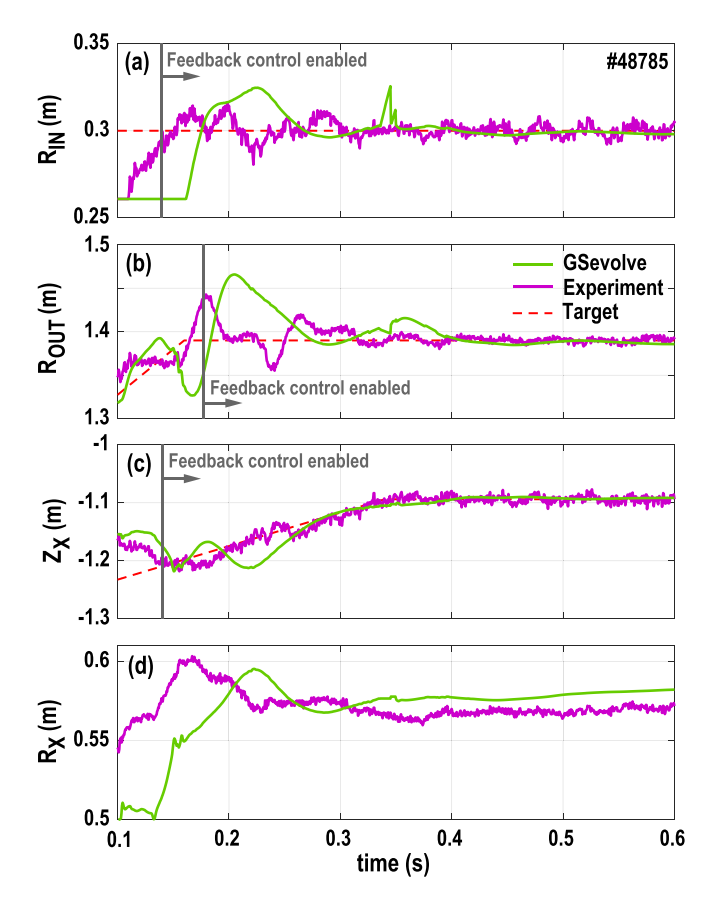


Figure 10. Control of plasma shape parameters R_{IN} , R_{OUT} , Z_X in a closed-loop GSevolve simulation and during the real experiment. R_X was not controlled, it is provided to demonstrate decoupling with other parameters.

5. Conclusions

In this manuscript we presented a magnetic equilibrium controller assessment framework developed for MAST-U. We demonstrated and validated the entire workflow, including the design, closed-loop simulations and evaluation of performance of magnetic controllers. This allowed development and implementation of qualified plasma shape controllers for a range of advanced MAST-U divertor configurations (such as super-X divertor, snowflake divertor, etc) with minimal experimental time. In many cases, just a few discharges were sufficient to test the controllers on-machine, and the remining control session time was devoted to the scenario optimization. This is a stark improvement compared to the previously used shape development approach based on trial and error through numerous discharges. Notably, this new approach is not limited to MAST-U but can be adapted to any existing or future tokamak.

Data availability statement

The data cannot be made publicly available upon publication because no suitable repository exists for hosting data in this field of study. The data that support the findings of this study are available upon reasonable request from the authors.

Acknowledgments

This material is based upon work supported by the U.S. Department of Energy, Office of Science, Office of Fusion Energy Sciences, under Award(s) DE-SC0018991, DE-SC0022272, DE-AC05-00OR22725, DE-AC52-07NA27344. This work has been carried out within the framework of the EUROfusion Consortium, part-funded by the European Union via the Euratom Research and Training Programme (Grant Agreement No 101052200 - EUROfusion) and from the EPSRC (grant number EP/W006839/1). To obtain further information on the data and models underlying this paper please contact PublicationsManager@ukaea.uk. Views and opinions expressed are, however, those of the author(s) only and do not necessarily reflect those of the European Union or the European Commission. Neither the European Union nor the European Commission can be held responsible for them.

Disclaimer

This report was prepared as an account of work sponsored by an agency of the United States Government. Neither the United States Government nor any agency thereof, nor any of their employees, makes any warranty, express or implied, or assumes any legal liability or responsibility for the accuracy, completeness, or usefulness of any information, apparatus, product, or process disclosed, or represents that its use would not infringe privately owned rights. Reference herein to any specific commercial product, process, or service by trade name, trademark, manufacturer, or otherwise does not necessarily constitute or imply its endorsement, recommendation, or favoring by the United States Government or any agency thereof. The views and opinions of authors expressed herein do not necessarily state or reflect those of the United States Government or any agency thereof.

ORCID iDs

A Lvovskiy https://orcid.org/0000-0002-3649-1169
H Anand https://orcid.org/0000-0002-9632-5680
A S Welander https://orcid.org/0009-0005-5063-7047
M Kochan https://orcid.org/0009-0007-9616-5828
C Vincent https://orcid.org/0000-0002-7227-409X
G McArdle https://orcid.org/0000-0003-0888-0105
J Lovell https://orcid.org/0000-0001-9565-3466
Z A Xing https://orcid.org/0000-0001-7768-5931
B Sammuli https://orcid.org/0000-0002-3000-9327
D A Humphreys https://orcid.org/0000-0002-0879-4074
N W Eidietis https://orcid.org/0000-0003-0167-5053
V Soukhanovskii https://orcid.org/0000-0001-5519-0145

A W Leonard https://orcid.org/0000-0001-9356-1074
A O Nelson https://orcid.org/0000-0002-9612-1936
J Harrison https://orcid.org/0000-0003-2906-5097

References

- [1] Fishpool G, Canik J, Cunningham G, Harrison J, Katramados I, Kirk A, Kovari M, Meyer H and Scannell R 2013 J. Nucl. Mater. 438 S356-9
- [2] Valanju P M, Kotschenreuther M, Mahajan S M and Canik J 2009 Phys. Plasmas 16 056110
- [3] Anand H et al 2024 Nucl. Fusion 64 086051
- [4] Soukhanovskii V A, Cunningham G, Harrison J R, Federici F and Ryan P 2022 Nucl. Mater. Energy 33 101278
- [5] Nelson A O et al (the MAST-U Team) 2024 Nucl. Fusion 64 124004
- [6] Harrison J R et al (the MAST-U Team and the EUROfusion MST1 Team) 2019 Nucl. Fusion 59 112011
- [7] Humphreys D A, Ferron J R, Hyatt A W, La Haye R J, Leuer J A, Penaflor B G, Walker M L, Welander A S and In Y 2008 Fusion Eng. Des. 83 193–7
- [8] Janky F, Fable E, Englberger M and Treutterer W 2021 Fusion Eng. Des. 163 112126
- [9] Carpanese F 2021 Development of free-boundary equilibrium and transport solvers for simulation and real-time interpretation of Tokamak experiments *PhD Thesis EPFL* Lausanne

- [10] Dnestrovskii A, Janky F, Medvedev S, Asunta O, Buxton P F and Nemytov V 2024 Recent progress with SOPHIA tokamak simulator for ST40 device 50th EPS Conf. on Plasma Physics (Salamanca, Spain)
- [11] Walker M L 2015 Development environments for Tokamak plasma control 2015 IEEE 26th Symp. on Fusion Engineering (SOFE) (Austin, TX, USA) pp 1–8
- [12] Walker M L, Welander A, Humphreys D, Ambrosino G, De Tommasi G, Bremond S, De Vries P, Snipes J, Rimini F and Treutterer W 2019 Fusion Eng. Des. 146 1853–7
- [13] McArdle G, Pangione L and Kochan M 2020 Fusion Eng. Des. 159 111764
- [14] Kochan M 2023 Real-time plasma shape reconstruction on MAST Upgrade based on local expansion 30th IEEE Symp. on Fusion Engineering (SOFE) (Oxford, UK)
- [15] Anand H, Eldon D, Kochan M, McArdle G, Pangione L and Wang H Q 2022 Fusion Eng. Des. 177 113086
- [16] Walker M L and Humphreys D A 2006 Fusion Sci. Technol. 50 473–89
- [17] Welander A S, Deranian R D, Humphreys D A, Leuer J A and Walker M L 2005 Fusion Sci. Technol. 47 763–7
- [18] Welander A, Olofsson E, Sammuli B, Walker M L and Xiao B 2019 Fusion Eng. Des. 146 2361–5
- [19] Welander A S, Wehner W P, Pajares A and Thome K E 2024 IEEE Trans. Plasma Sci. 52 3898–903